Available online at www.sciencedirect.com

ScienceDirect

Energy Procedia 49 (2014) 2145 – 2153

Energy Procedia

SolarPACES 2013

A new instrument for measuring the reflectance distribution function of solar reflector materials

S. Meyen[a,]*, F. Sutter[a], P. Heller[a], A. Oschepkov[a]

[a] *DLR German Aerospace Center, Institute of Solar Research, PSA, Ctra. Senés Km. 4, P.O.Box 44, 04200, Tabernas, Almería (Spain)*

Abstract

During the last years, the importance of correctly measuring the reflectance properties of solar reflector materials has increased due to the fact that more and more different kinds of materials compete on the market. Customers and manufacturers likewise need reliable tools to ensure the quality of the reflector and evaluate its performance in the desired concentrated solar power (CSP) application. The SolarPACES Reflectance Measurement Guideline [1] defines the parameters that are necessary for a thorough reflector qualification. The work on this guideline made it evident, that the state of the art of measurement technology is not sufficient for measuring all of these parameters in the ideal way. For some reflector materials, this can lead to improper estimations of their reflectance characteristics and their performance. Until now it was not possible to measure the most important parameter, the specular reflectance, $\rho_s(\lambda,\theta,\varphi)$, in the ideal format as a function of wavelength, λ, acceptance angle, φ, and incidence angle, θ. The currently most common method is to measure $\rho_s(\lambda,\theta,\varphi)$ at few selected φ and λ and to estimate the solar weighted specular reflectance, $\rho_s(SW,\theta,\varphi)$. One solution is the measurement of the bidirectional reflectance distribution function (BRDF) and use it to calculate $\rho_s(\lambda,\theta,\varphi)$ as a function of φ and θ. At the OPAC laboratory a new instrument MIRA (Mirror Reflectance Function Analyzer) was developed that offers the possibility to measure the bidirectional reflectance distribution of the light reflected by a mirror into the hemisphere at variable incidence angles [2]. In advantage to traditional goniometers or gonioreflectometers of which only few reach the necessary angular measurement resolution, MIRA uses a time saving technique and occupies comparably little space that is available in any laboratory. The instrument allows measurements at different selected wavelengths for the approximation of the solar weighted specular reflectance. This paper gives a detailed description of the instrument prototype and first preliminary measurement results are compared with a reference measurement. The instrument design and data evaluation method has a German patent [3].

Selection and peer review by the scientific conference committee of SolarPACES 2013 under responsibility of PSE AG.
Final manuscript published as received without editorial corrections.

* Corresponding author. Tel.: +34 950 611 743; fax: +34 950 260 315.
E-mail address: Stephanie.Meyen@dlr.de

Selection and peer review by the scientific conference committee of SolarPACES 2013 under responsibility of PSE AG.
Final manuscript published as received without editorial corrections.
doi:10.1016/j.egypro.2014.03.227

Keywords: Solar reflector; specular and hemispherical reflectance; scattering; reflectance distribution function; goniometer

1. The basic measurement principle

MIRA is based on the principle of a Coblentz sphere [4] and on an idea published in 1992 [5] with significant changes to fulfill the special requirements of its application in the CSP industry. The mirrored ellipsoid of the MIRA has two focal points (see Figure 1) where the sample and the detector are placed. The distance between the center and one of the focal points is called excentricity. The instrument takes advantage of the fact, that every light ray coming from one focal point is redirected by the reflective walls of the ellipsoid to the other focal point. The ellipsoid works similar to other imaging systems and thus light rays originating at a small distance to the focal point are projected equally distant to the second focal point. This leads to the characteristic, that a collimated light bundle is focused by the ellipsoid at a distance that corresponds to approximately half its small half-axis length (see the latent image in Figure 1). A sample mirror is positioned in the 1st focal point and illuminated by collimated light. After reflection on the sample, the light is then also reflected by the ellipsoid wall and travels to the 2nd focal point, where a camera with a 180° fisheye lens captures it. The object distance of the lens is set to half the distance of the small half-axis to capture the latent image. Every pixel on the CCD represents one latent-image-focus, each of which corresponds to one angle direction in which the light left the sample. Thus the angular resolution of the instrument depends on the number of pixels and the fill factor (the amount of space between pixels that is not light sensitive related to the pixel size). A perfectly specular mirror reflects the collimated incident light in only one single (the specular) direction and therefore produces a small spot image on the CCD. This is the instrument signature. Any scattering sample reflects the collimated incident light in more than one direction and produces a larger image corresponding to the scattering angles in which the light rays left the sample (Figure 1). From the intensity distribution on the CCD, the reflected beam distribution at the sample can be derived.

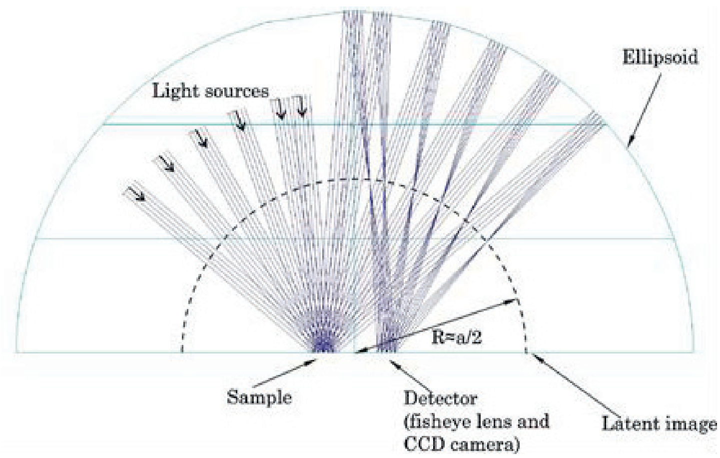

Figure 1: Raytracing model of beam paths

2. MIRA prototype

The scheme of the prototype instrument MIRA is shown in Figure 2. It was decided on using aluminum as material after a thorough investigation on possible degradation and deformation problems. The manufacturer and also experts on aluminum coated telescope mirrors confirmed that the comparably constant environmental conditions of an enclosed body in a laboratory are sufficient protection against degradation. These conditions also suggest little probability for deformation based on drastic temperature changes. In a first step the ellipsoid has been milled from an aluminum block. Secondly the inner surface has been polished with a diamond milling head to reach the precise shape and low surface roughness for a high specular reflectance of the ellipsoid walls. For its functioning, the precision of the ellipsoid shape is crucial and needs to achieve a diversion of no more than 0.5 mrad to the ideal surface normal at any point. Imperfections in shape would mainly result in a redirection of the light beam hitting on this part of the ellipsoid in a different direction than desired and misses the entrance pupil of the lens, respectively is not redirected towards the second focal point. The manufacturing of the ellipsoid was a challenge because of its large size and its precision requirements. It was machined on the edge of the technically feasible. To ensure the shape precision of the finished piece, the inner surface was inspected with a tactile measurement device by the manufacturer. After seeing the first measurement results (see section 4), a different approach to inspect the ellipsoid shape is under development.

The ellipsoid is covered with a lid which contains two openings, one for the camera and one for the sample holder. The position of the sample holder can be adjusted in all directions with three precision screws so that the incidence beam hits the reflective plane of the sample exactly in the focal plane of the ellipsoid. A tool for performing this positioning precisely is still under development. Once the precision screws have been adjusted correctly (i.e. before a measurement session) they do not need to be touched again when changing a sample, except when the position of the reflective plane in the sample changes (i.e. different glass thickness). The CCD camera is equipped with a fisheye lens that has 180° field of view and produces an undistorted, circular image of the hemisphere onto the CCD. The linearity of the sensor and low noise level has been tested. For illumination, a white light source is coupled into a fiber and collimated using a reflective collimator. The beam has a diameter of 6 mm. Different filters can be placed in front of the white light source in order to take measurements at several wavelengths and polarization directions. The collimator sits on a rail circumventing the outer hull of the ellipsoid, so that the position of the light source is adjustable for incidence angles in the range of 6.5° to ~40° with a precision of ± 1° (see Figure 3). A very important detail of the instrument is a shadow strip (see Figure 2), which can be positioned along the inner ellipsoid wall to block the main specular reflex. This way the scattered radiation is made visible using a longer integration time. The whole prototype has been set up in the OPAC laboratory at the Plataforma Solar de Almería within a light proof housing that protects it from straylight and dust pollution.

Technical data about the prototype instrument are shown in Table 1.

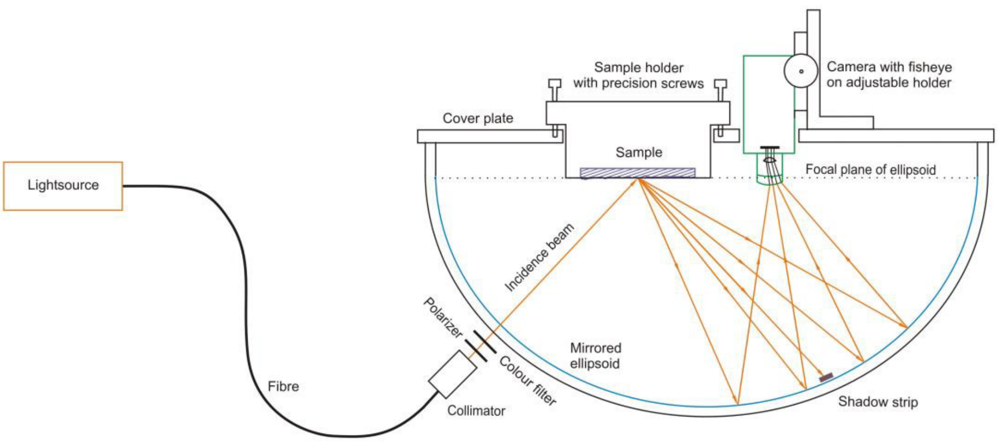

Figure 2: Scheme of instrument

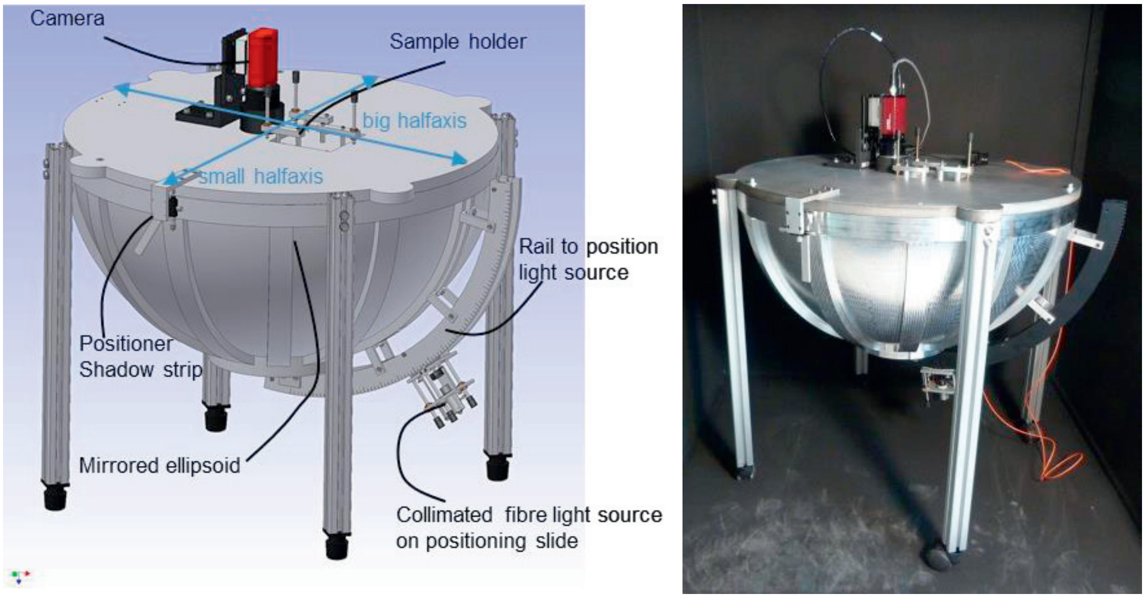

Figure 3: Construction sketch of instrument and mounted prototype

Table 1: Technical data of the MIRA prototype

Ellipsoid data	
Approx. dimensions of ellipsoid	Diameter: ca. 700 mm; Height: ca. 345 mm
Minimum angle of incidence	6,5°
Theoretical angular resolution of measurement	1.3 msr/pix or 0.95 mrad/pix in plane of small axis and 1.27 mrad/pix in plane of big axis
Maximum sample size	100 x 100 mm
Illumination	
Spot diameter	6 mm
Collimation	1.64 mrad full angle divergence (= 0.094°, maximum acceptable is 0.095°)
Different wavelengths are realized with interference filter	400, 450, 500, 550, 600, 650, 700, 850 and 940 nm
Band width FWHM	10 nm
Camera	
Spectral sensitivity	400-1000nm
Pixel	3296 x 2472 (8Mpixel)
Fillfactor	80%
Pixelsize Dynamic range	5.5 x 5.5 µm 14 bit
Focal length	f = 4.5 mm
f-number in use	k = 2.8 (D_{EP} ~ 2mm)
Angle of view	180°

3. Data acquisition and image analysis

A measurement of a mirror sample with MIRA consists basically in taking three images. The first image is taken at short exposure time (see Figure 4a). The exposure time is set manually by the operator in order to avoid overexposure of the central peak. Measuring an ideal mirror sample without any scattering and supposing an aberration-free instrument, the result would be an image with just a single illuminated pixel. In reality, imperfections of the ellipsoid wall, the collimation of the light source and aberrations of the fisheye lens make the image a little bit wider even for a very good specular mirror (see Figure 4a). The properties of the CCD give MIRA an angular resolution of 1.2 mrad per pixel. This means that light detected within a circle with a radius of 10 pixel corresponds to reflectance at 12 mrad acceptance angle. Any scattered light coming from a less specular sample will be captured by the pixels surrounding the peak, with less intensity. To measure this, a second image is taken with long exposure time and using a shadow strip that covers the main reflectance peak. This allows the measurement of the scattered distribution with a high signal to noise ratio (see Figure 4b). The shadow strip is manually positioned by the user to cover the main peak of the reflected light (the manual lever is shown in Figure 3). Not using the shadow strip to detect the scattered distribution would result in overexposure of the specular peak and camera chip blooming (see Figure 4c). Blooming occurs when the charge in a pixel exceeds the saturation level and the charge starts to fill adjacent pixels. Because the shadow strip covers a whole strip in the hemisphere and not only the specular peak, a third image is taken with the sample rotated by 90 degrees compared to the second image. This is required to detect anisotropic reflectance behavior. Combining the images after adapting the grayvalues to matching integrating times (see section 4) gives the distribution of the peak together with the scattered part (Figure 5c).

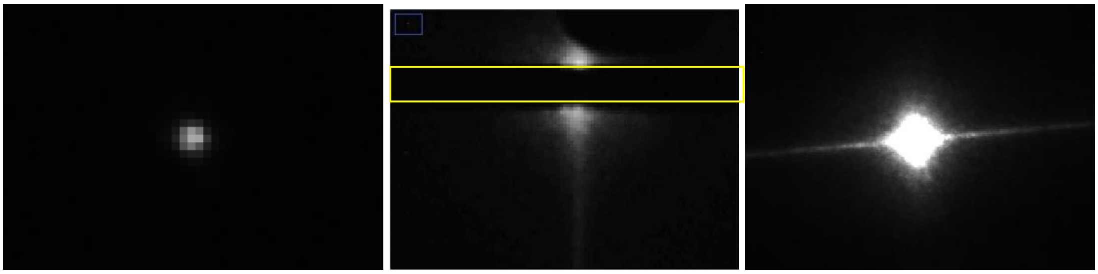

Figure 4: a) specular peak of aluminum mirror (short exposure time), b) diffuse part (long exposure time), specular peak is covered by shadow strip (indicated by yellow box), c) blooming of camera chip due to long exposure time not using shadow strip

After image processing of the three measurement images, the BRDF for one incidence angle is computed. *Matlab* is used for the data treatment. The first step in the image processing is to stitch the three images together after a dark noise image has been subtracted. Pixel covered by the shadow strip will be replaced by the intensity values from the other images. It needs to be taken into account that the image containing the specular peak has been taken at a shorter exposure time and thus two equal gray values in the three images do not represent equal reflected intensities. A correction of the image with short exposure time is performed taking advantage of the linearity of the CCD. Preliminary tests with a stable light source showed a linear correlation between exposure time and gray value. Applying the following formula, the gray value of each (short exposed) pixel that is stitched into the longer exposed image is computed:

$$GP_{transformed} = GP_{meas} \cdot \frac{t_{Shadow}}{t_{Peak}}$$

where $GP_{transformed}$ is the theoretical gray-value for the peak measurement corresponding to the exposure time from the measurement with shadow strip t_{Shadow}, GP_{meas} is the measured gray-value from the peak measurement and t_{Peak} is the exposure time from the peak measurement. This way the peak measurement intensity is significantly higher than the shadow measurement. Figure 5c demonstrates that this approach connects well peak and scatter measurement.

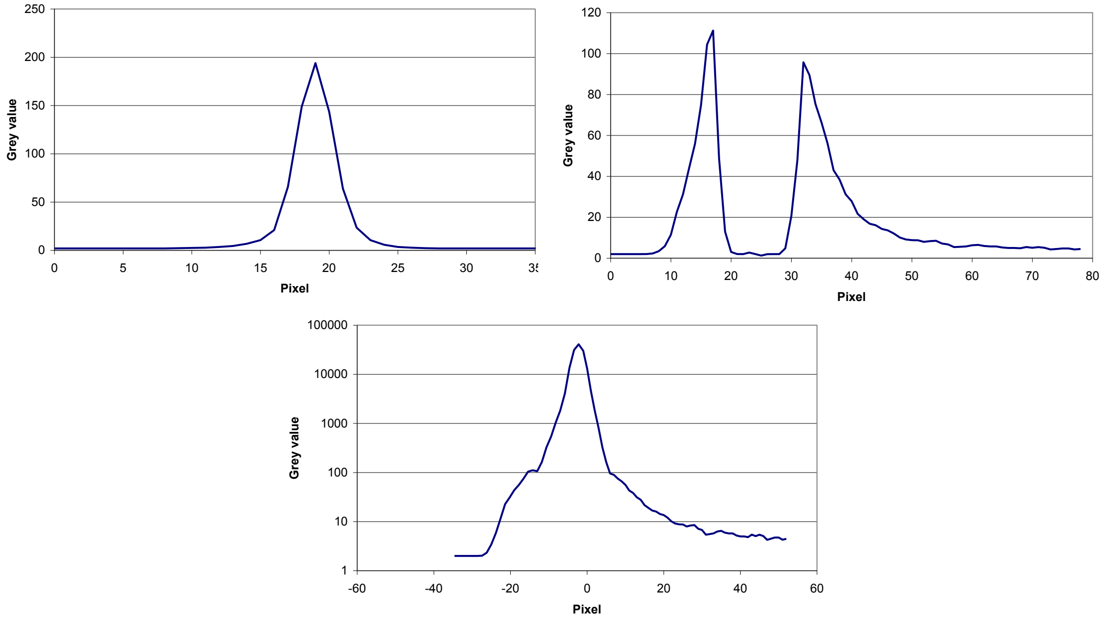

Figure 5a: Intensity distribution along a line crossing the peak; b) Intensity distribution along a line crossing the peak with shadow strip in the up-down direction on Figure 4b (the left part of the distribution is influenced by the opening in the ellipsoid for the incident light); c) Stitched intensity distribution of a) and b) after conversion of the peak measurement to match the integration time of the shadow strip measurement.

Once the images have been stitched, the thus generated measurement image can be used to compute the reflectance distribution. The pixel containing the maximum of the reflectance peak is detected and defined as the center of a polar coordinate system. Then the Cartesian coordinates of the pixels must be converted into polar coordinates of the intensity distribution around the maximum peak. In preliminary tests with reflective gratings that reflect collimated light in defined angles it was shown that a correlation between the angle of the light reflected from the sample (grating) and the pixel position confirms the theoretical measurement resolution of 1.2 mrad/pixel for the whole hemisphere respectively sensor area. An array is created which links the Cartesian coordinate of each pixel to the corresponding elevation and azimuth angle together with the measured intensity at this point. The result is an intensity distribution similar to the example shown in Figure 6.

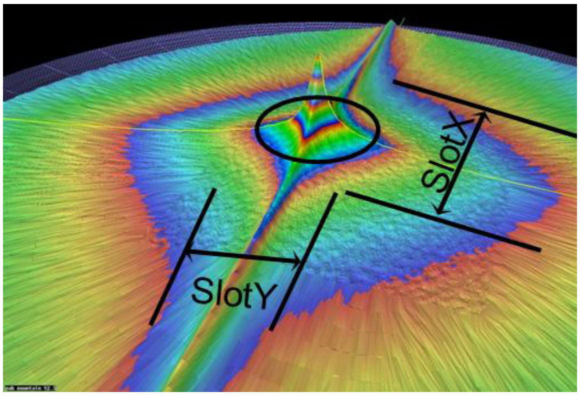

Figure 6: BRDF of an aluminum reflector and different apertures [source: *pab* measurement results]

The integrated intensity from all pixels corresponds to the hemispherical reflectance value of the sample, which needs to be measured for example with a spectrophotometer. The last step of data treatment consists in performing a Delaunay triangulation for the integration of grey values. Starting at the center of the peak, a virtual aperture with a stepwise expanding radius representing different acceptance angles is used to calculate the specular reflectance for each acceptance angle step to result in the specular reflectance as a function of acceptance angle. Repeating the process at other wavelengths or incidence angles gives all information needed.

4. First measurements

The MIRA prototype has been set up and first measurements have been taken with different mirror types. Beforehand, the same samples had been sent to *pab Advanced Technologies Ltd.* for a measurement of the BRDF with their Gonio-Photometer at $\lambda = 633$ nm for reference [5]. Particularly for solar mirrors it makes sense to define virtual apertures encircling the peak reflectance in order to measure the dependency of specular reflectance and acceptance angle. With the measured data this dependency is easily computable. Also, linear apertures might be useful to characterize non-isotropic reflective materials employed for line focusing systems like parabolic troughs (see aluminum reflector in Figure 6. A higher intercept factor might be achieved when the reflector is mounted so that the absorber tube is parallel to the direction of the aperture Slot Y). The possibility to measure the reflectance within variable linear and circular apertures has been implemented in the *Matlab* code.

The measurement results have been compared with the data generated by *PAB Advanced Technologies Ltd*. The results show good agreement at acceptance angles bigger than 10 mrad (see Figure 7). However, for smaller acceptance angles there are significant deviations. The MIRA measurement of a highly specular thin glass mirror already shows a much broader peak than the *pab* measurements of reflectors with less specularity, although this is not expected for this kind of mirror. This indicates that the instrument signature in itself does not allow to distinguish the distribution at small acceptance angles. Reasons for this are being investigated at the moment. The problem might be due to manufacturing errors of the ellipsoid like imperfections in the shape of the ellipsoid wall or scattering effects at the surface. Deviations might also be induced by the not perfectly collimated light source or erroneous sample holder position respective to the camera so that no exact match with the focal points of the ellipsoid is achieved. These effects will be studied and improved in the future in order to achieve a higher measurement precision in the small acceptance angle range. Positioning will be improved and if possible, correction functions will be applied to the measurement image to minimize the offset for small acceptance angles.

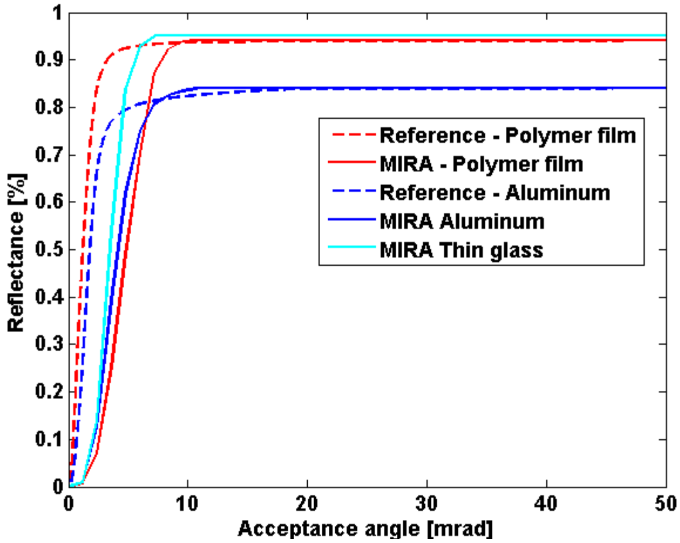

Figure 7: Comparison of the measurement data from MIRA with data generated with the goniometer from *pab,* circular acceptance aperture, 15° incidence angle, wavelength 650 nm

5. Conclusions and outlook

State of the art reflectance measurement technology is not sufficient to fulfill the requirements for an ideal reflector characterization as defined in the SolarPACES reflectance guideline. The different concentrating solar technologies demand high reflectance at specified acceptance angle ranges from the reflector materials. Knowledge of the BRDF allows computing the specular reflectance as a function of acceptance angle. These data can be used to select the most appropriate mirror material for each concentrating technology and to evaluate its performance. A novel, time-saving method to measure the BRDF of solar mirror materials has been presented. An instrument prototype has been set up and first measurements have been compared with reference measurements. The instrument results showed good agreement with a goniometric reference measurement for acceptance angles larger than 10 mrad. It has been demonstrated, that the measurement principle and data evaluation is viable and that the knowledge of the BRDF serves well for computing $\rho_s(\lambda,\theta,\varphi)$ as a function of φ. Further work is planned in order to improve the measurement precision at smaller acceptance angles. MIRA offers a new alternative to state of the art instruments for measuring the specular reflection properties, with the benefits of measuring also at selectable λ and θ.

Acknowledgements

The authors want to thank Martin Hagmann, Arantxa Fernandez-Garcia and Lucía Martinez from the OPAC laboratory from the Centro de Investigaciones Energéticas, Medioambientales y Tecnológicas (CIEMAT). Thanks also to Dr. Peter Apian-Bennewitz from *pab* and to the German Ministry of Environment, Nature Conservation and Nuclear Safety (BMU) for the project funding.

References

[1] SolarPACES Reflectance Guideline. Parameters and Method to Evaluate the Solar Reflectance Properties of Reflector Materials Concentrating Solar Power Technology – Version 2.5. http://www.solarpaces.org/Tasks/Task3/reflectance_guideline.htm; June 2013

[2] Martin Hagmann. Analysis of the Reflection Properties.of Solar Mirror Materials by Measuring the BRDF to Enhance the Precision of State of the Art Methods. Diploma Thesis. Karlsruhe Institute of Technology; May 2012

[3] German Patent DE 10 2012 214 019.0. Photogoniometrisches Reflektometer - Mirror Reflectance Function Analyzer (MIRA)

[4] ASTM 1048-87. Standard Test Method for Measuring the Effective Surface Roughness of Optic Components by Total Integrated Scattering.

[5] Gregory J. Ward. Measuring and Modeling Anisotropic Reflection. Siggraph '92 Chicago, July 26-31, Computer Graphics 26, 2, July 1992

[6] pab Advanced Technologies Ltd web flyer. Gonio-Photometer for reflection & transmission measurements. www.pab.edu.